

## A mode coupling theory analysis of viscoelasticity near the kinetic glass transition of a copolymer micellar system

This article has been downloaded from IOPscience. Please scroll down to see the full text article.

2004 J. Phys.: Condens. Matter 16 S4975

(<http://iopscience.iop.org/0953-8984/16/42/013>)

View [the table of contents for this issue](#), or go to the [journal homepage](#) for more

Download details:

IP Address: 129.252.86.83

The article was downloaded on 27/05/2010 at 18:21

Please note that [terms and conditions apply](#).

# A mode coupling theory analysis of viscoelasticity near the kinetic glass transition of a copolymer micellar system

Francesco Mallamace<sup>1,2</sup>, Piero Tartaglia<sup>3</sup>, Wei Ren Chen<sup>1</sup>,  
Antonio Faraone<sup>1,2</sup> and Sow Hsin Chen<sup>1</sup>

<sup>1</sup> Department of Nuclear Engineering, Massachusetts Institute of Technology, Cambridge, MA 02139, USA

<sup>2</sup> Dipartimento di Fisica and INFN, Università di Messina, I-98166, Messina, Italy

<sup>3</sup> Dipartimento di Fisica, INFN and Statistical Mechanics and Complexity Center, Università di Roma La Sapienza, I-00185 Rome, Italy

Received 22 April 2004

Published 8 October 2004

Online at [stacks.iop.org/JPhysCM/16/S4975](http://stacks.iop.org/JPhysCM/16/S4975)

doi:10.1088/0953-8984/16/42/013

## Abstract

We report a set of viscoelastic measurements in concentrated aqueous solutions of a copolymer micellar system with short-range inter-micellar attractive interactions, a colloidal system characterized, in different regions of the composition–temperature phase diagram, by the existence of a percolation line (PT) and a kinetic glass transition (KGT). Both these transitions cause dramatic changes in the system viscoelasticity. Whereas the observed variations of the shear moduli at the PT are described in terms of percolation models, for the structural arrest at the KGT we investigate the frequency-dependent shear modulus behaviours by using a mode coupling theory (MCT) approach.

## 1. Introduction

Soft and complex materials (polymers, proteins, polyelectrolytes, foams, granular materials, colloids, etc) are of great interest in many different areas of pure science and technology. As it is well known, they are characterized by a hierarchical structural order, in the mesophase scale, that gives rise to a dynamical behaviour characterized by multirelaxations that span many different temporal orders of magnitude. The origin of these phenomena is in the interparticle interaction that, in the same system, depending on the thermodynamical variables (temperature, composition, pressure) can give rise to a large variety of metastable or stable structural orders and phases.

Among the many complex fluids constituting soft matter, colloids are a model system for the reason that they present unique features: their interaction potential is in general short ranged (i.e., small if compared with the typical particle sizes) and, in addition, the ratio between the

repulsive and the attractive contribution can be easily modelled [1]. Therefore, with the change of the interparticle interaction colloids exhibit a rich variety of phase behaviours including ordered crystalline structures. The existence of a liquid–liquid phase demixing line with a critical point and a percolation transition line [2, 3] is typical of these systems. These latter phenomena, that cover a wide range (in the temperature–composition plane), can be traced back to the short-range nature of the interaction potential.

However, among the different phases that colloidal systems can have, the most interesting is the existence of glassy states (structurally arrested (SA) or jammed states) [4, 5]. These are amorphous states of matter that cannot be categorized as gaseous, liquid or crystalline. In soft materials this jamming, where the system particles are caught in a small region of phase space with no possibility to escape, has been usually obtained under appropriate density and load conditions. Examples are hard sphere colloids, where the SA is obtained by changing the particle packing fraction (or volume fraction  $\phi$ ) [5], or granular matter, where the arrest is obtained by using the load as order parameter [6]. Recently, considering colloids with attractive interaction, an intriguing ‘theoretical speculation’ [7] proposes a ‘general’ phase diagram for the SA for which attractive particles may undergo a fluid-to-solid transition driven by several order parameters: density, load and an effective temperature ( $T^*$ ) directly related to the magnitude of the attractive interparticle energy ( $u$ ) [8]. On these bases the SA in soft materials seems to show hallmarks of universality and the addressing of these new conceptual problems related to attractive colloids represents today one of the most challenging subjects of statistical physics. New and known approaches have been used, and in particular the mode coupling theory (MCT) led to important suggestions [9–11], which were explored by different experimental techniques.

In the past a number of theoretical approaches based on thermodynamical concepts have been proposed to interpret the SA. Examples include the percolation and liquid-to-solid transitions [12]. However, none of these models was satisfactory compared with experimental evidence, whereas idealized MCT gains significant results for systems in which the colloidal particles can be modelled as hard spheres (HSs) [5]. The major MCT predictions can be summarized as follows at low  $\phi$ , the system behaves as a fluid. As the volume fraction increases, the density–density correlation function (or intermediate scattering function (ISF)) exhibits a two-stage relaxation process: the initial ISF decay, that corresponds to the rattling of a particle confined within a transient cage formed by its neighbours, is followed by a slow decay resulting from the cage relaxations and the escape of the trapped particles by the re-arranging of their nearest-neighbour configurations. This latter process, collective in character, leads to a particle diffusion coupled to the structural relaxations. The system dynamics becomes slower when  $\phi$  is near a certain ‘critical’ value ( $\phi_c$ ), beyond which the system will be ‘arrested’ in an amorphous state, rather than condensing into a crystal. From this MCT viewpoint, the system transition in the amorphous glass state is considered as a critical one in nonergodic states (with  $\phi - \phi_c$  as the separation parameter and the ISF time behaviour governed by precise scaling laws) and in addition the SA transition is the consequence of a kinetic glass transition (KGT). Experiments have confirmed the successful application of KGT to HS colloids and its main features, although they have also proposed some dynamical behaviours which cannot be interpreted in the frame of the HS potential alone.

Recently, considering colloids with attractive interactions, MCT calculations propose a new SA scenario that confirms the theoretical suggestions of a KGT driven also by an effective temperature  $T^*$ . On the basis of these new MCT approaches for adhesive hard-sphere systems (AHSs), the corresponding phase behaviour is characterized by  $T^* = k_B T/u$ , the volume fraction of the particles  $\phi$  and the fractional attractive well width  $\epsilon = \Delta/R$ , where  $-u$  is the depth of the attractive square well (or the magnitude of the attractive interparticle energy),

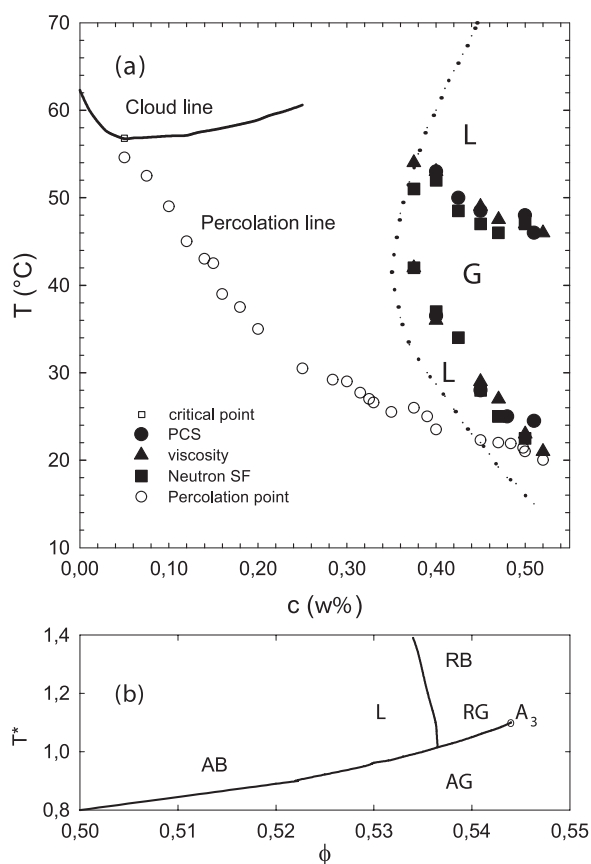


**Figure 1.** (a) The phase diagram (in the  $T$ - $c$  plane) of Pluronic L64 three-block copolymer in  $\text{D}_2\text{O}$  solutions. The phase diagram contains the cloud point line, the percolation line [21], the equilibrium liquid-to-crystal phase boundary (dotted-dashed line) and the re-entrant kinetic glass transition line (KGT) lines, which are determined by PCS, SANS, and shear viscosity measurements. (b) The theoretical phase diagram (in the  $T^*$ ,  $\phi$  plane) determined by mode coupling theory for a colloidal system with a short-range attractive square-well potential ( $\epsilon = 0.03$ ) [9].

$\Delta$  the width of the well and  $R$  the particle diameter. Therefore, the loss of ergodicity can be driven either by increasing  $\phi$  or by changing  $T^*$ . The bottom panel of figure 1(b) gives part of the MCT predicted phase diagram on the AHS with  $\epsilon = 0.03$ . Contrarily to MCT results for HS where the KGT is explained in terms of cage effects [4] (with volume fraction ( $\phi$ ) as the only control parameter), for AHSs the new and rich physical scenario that arises is mainly due to clustering processes and the corresponding phase diagram ( $\phi$ ,  $T$  dependent) is due to the competition between cage and clustering processes [9–11]. As can be observed, depending on the control parameters, the AHS colloids are characterized by (i) a liquid region (L); (ii) two kinetic glass transition lines, one corresponding to the HS glass at high composition (repulsive branch (RB)) and the other one extending to much lower concentrations (attractive branch (AB)). The former is attributed (with the usual mechanism due to excluded volume) to the repulsive part (repulsive glass (RG)) of the interaction, the latter (temperature dependent) to the attractive part of the potential (attractive glass (AG)); (iii) a cusplike singularity with a glass–liquid–glass re-entrant behaviour; (iv) an AG–RG transition line, starting where the AB crosses the RB, ending in a point of type  $A_3$  [4]. Therefore, new phenomena arise:

- (a) Near the AG–RG transition density, correlation functions exhibit a logarithmic time dependence followed by a power-law behaviour, before the structural arrest takes place [4]. This logarithmic dependence (the limiting case of a power law with a vanishing exponent) is due to the existence of higher order glass transitions of type  $A_3$  [13] or  $A_4$  [10].
- (b) The system can undergo a re-entrant (glass-to-liquid-to-glass) and a glass-to-glass transition by varying  $T^*$ .
- (c) At the  $A_3$  singularity the glass-to-glass transition line terminates and the long time dynamics of these two distinct SA states become identical at and beyond this point.

Several experimental studies, by using polymer grafted colloids (in which attraction is originated by the depletion interaction) [14, 15] and dense micellar systems, have confirmed some of these MCT predictions, such as the re-entrant glass-to-liquid-to-glass and glass-to-glass transitions, as well as the logarithmic relaxation near the  $A_3$  point [16, 17]. In particular, in a series of different experimental investigations, by using dense three-block copolymer micelles, we have reported a detailed analysis on the physical properties of these two glassy states (AG and RG) [18, 19]. The agreement between our data on L64/D<sub>2</sub>O micelles and MCT was satisfactory on a quantitative level, so that the system whose phase diagram (in a  $T$ – $\phi$  plane) is shown in the top panel of figure 1(a) can be usefully treated in the framework of MCT.

As it can be observed the L64/D<sub>2</sub>O phase diagram, in addition to the re-entrant KGT lines in the high composition region, is characterized by a well defined percolation line (PT) that spans the temperature composition plane in a large concentration interval ( $0.05 < c < 0.52$  wt%). This line has been determined by photon correlation spectroscopy and rheological data [20]. Certainly the short-range attraction is the ideal ingredient for the existence in the same system of the liquid–liquid demixing line, of the percolation transition line [2, 3] and of the KGT behaviours predicted by MCT. In fact, the basic idea underlying the explanation of these phenomena is the clustering process [11]. In certain thermodynamical states, attractive colloids tend to form polydisperse aggregates, some of which may span the whole sample (the percolation cluster) and, traditionally, the resulting sol–gel transition is entirely described by means of a percolation transition (PT) [21]. Instead, the kinetic glass transition (KGT) in AHS colloids is described by MCT through the formation of the attractive glass in which the motion of the typical particle is constrained by the clustering formation with neighbouring particles. Originally, the KGT in AG has been interpreted in terms of static percolation [22], but the interpretation along this line did not agree with experiments. In fact figure 1 shows the SA in a phase diagram region different from the one where the gelation occurs. However, it is of interest to study the possible interplay between these two mechanisms, percolation and KGT, both due to the clustering process originated by the interparticle attraction. The way to obtain insight on this intriguing situation is to study the system viscoelasticity: an experimental approach that is strongly sensitive to the changes of the mechanical properties when the system evolves from a liquid to a solid-like behaviour.

Hence, we discuss the complex frequency-dependent viscosity in the L64/D<sub>2</sub>O micellar system previously studied in a different experiment to account satisfactorily for the MCT suggestions in AHS colloids. The main result is the possibility of interpreting the shear moduli, in the phase region of the KGT, in the framework of the MCT. Whereas viscoelasticity at PT [21] in complex fluids has been well studied [23, 24] (and also constitutes now the subject of deeper investigations), only limited attention was devoted to shear moduli close to the KGT in colloidal systems. Recently, the way in which the KGT affects the linear viscoelasticity has been investigated [8] in HS colloids for various volume fractions  $\phi$ . As one approaches the KGT, the evolution of the system structure results in a strongly concentration

and frequency dependent contribution to both the storage  $G'(\omega)$  and loss  $G''(\omega)$  shear moduli. The experimental data have been successfully treated by combining MCT with the contribution of Brownian motion. The main hypothesis is that the current fluctuations giving rise to the complex viscosity are related to the density correlation function and can be described by the so-called  $\beta$ -correlator of MCT. In our case, an AHS system, the use of an additional control parameter such as temperature, beside volume fraction, is therefore necessary and will be properly introduced. These considerations, together with the general findings of MCT, applying to attractive colloids and many recent experiments on the KGT in micellar systems, constitute the basis of the present study in which we explore the  $T$  dependence of viscoelasticity near the KGT line.

## 2. Experimental details

The system we study, called L64, is described in detail in [20]. It is an aqueous solution of a non-ionic three-block copolymer made of polyethylene and polypropylene oxides, [(PEO)<sub>13</sub>–(PPO)<sub>30</sub>–(PEO)<sub>13</sub>], having a molecular weight of 2990 Da. The main property of the copolymer molecules is that in water they are  $T$  dependent surfactants that spontaneously form hydrated monodisperse spherical micelles in a wide  $T$ – $c$  range. At low temperatures, both PEO and PPO are hydrophilic, so that the L64 chains readily dissolve in water, and the polymer exists as unimers. However, increasing  $T$ , PPO tends to become less hydrophilic than PEO, creating an unbalance in the hydrophilicity between the central block and the end-block of the polymer molecules, that consequently acquire surfactant properties and self-assemble to form micelles. The intermicellar attraction is mainly due to the fact that, on further increasing  $T$ , water becomes progressively a poor solvent to both PEO and PPO chains. The evidence of the short-range attraction is the system phase diagram, characterized by an inverted binodal curve with a lower consolute critical point ( $c_c = 5$  wt%;  $T_c = 330.3$  K), a  $T$ – $c$  dependent PT line cutting across the phase diagram, starting from the vicinity of the critical point to at least 55 wt%, and finally the  $T$ – $c$  dependent KGT line [16]. Samples were prepared by using a standard procedure with a proper purification in order to remove hydrophobic impurities and then dissolved in deuterated water [20].

Measurements of the storage modulus,  $G'(\omega)$ , and of the loss modulus,  $G''(\omega)$ , as a function of  $T$  at different  $c$ , were performed with a strain-controlled rheometer using a double-wall Couette geometry, in the frequency range  $0.0924 < \omega < 60$  rad s<sup>−1</sup>. To ensure a linear response, for the different working  $T$  (in a stability range of  $\pm 0.01$  °C) and  $c$ , we have tested our system as a function of low applied strains  $\gamma$ . After this check a low strain deformation,  $\gamma = 0.05$ , was maintained for all the experiments. In such a condition viscosities were measured in the shear rate range of  $0, 3 < \dot{\gamma} < 10$  s<sup>−1</sup>; this corresponds to Peclet numbers  $Pe < 1$ , where  $Pe = \dot{\gamma}\xi^2/2D_0$  characterizes the amount of distortion of structures with linear dimension  $\xi$  ( $D_0$  is the particle short-time diffusion coefficient at low concentration where hydrodynamic effects dominate). These distortions are responsible for shear thinning in the system structures, which is expected to set in at  $Pe \approx 1$ . In other words, such a condition constitutes an important experimental constraint in the study of the elasticity of systems characterized by clustering processes such as polymer solutions and attractive colloids. This is also very important for viscosity measurements in phenomena dominated by long-range ‘critical’ correlations such as those which originate the diverging incipient cluster typical of the percolation threshold in the sol–gel transition. Just in these processes, shear thinning can originate a ‘levelling off’ of the measured viscosities. In fact, in contrast to atomic or molecular liquids, complex fluids are characterized by diverging long-ranged structures able to support energy storage and hence an increase in the elastic component; this dramatically affects their

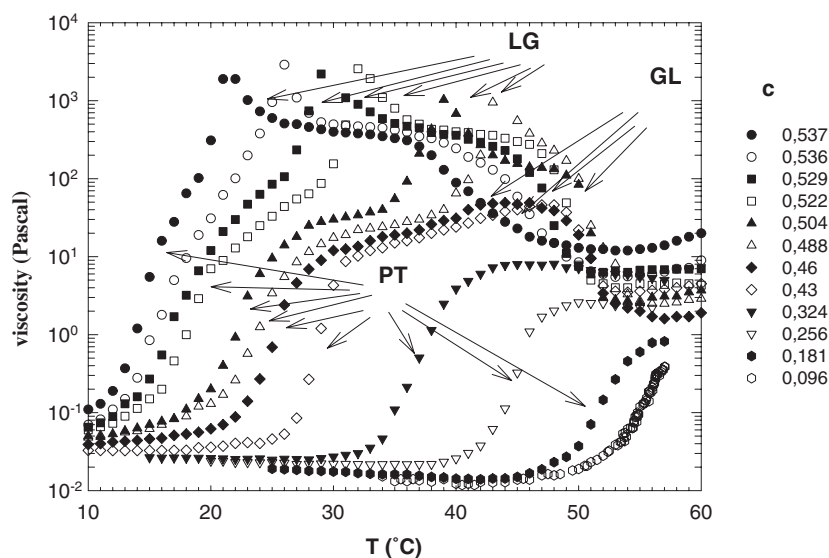


**Figure 2.** The zero-shear viscosity at 12 different concentrations as a function of temperature. Starting from low temperatures, the shear viscosity increases steeply, first going through a percolation transition (PT), then to a liquid-to-glass transition (LG) and finally a glass-to-liquid transition. Note that for concentrations  $c < 0.4$  there is only the percolation transition.

viscoelasticity. For example, as temperature (and concentration) approaches the percolation threshold, the structure of the suspension results in a strong frequency (or concentration) dependence of both  $G'(\omega)$  and  $G''(\omega)$ .

### 3. Results and discussion

We start considering the measured zero-frequency viscosities of the L64/D<sub>2</sub>O system at different concentrations as a function of temperature. Typical results are shown in figure 2. The low shear viscosity at all concentrations ( $0.095 < c < 0.537$ ) is characterized by an initial increase, starting from viscosity values typical of the solvent ( $\eta \sim 10^{-2}$  Pa) followed by a flattening off at the highest temperatures. At low concentrations,  $0.095 < c < 0.32$ , it can be observed that the micellar solution behaves like a simple fluid; for a large temperature interval its shear viscosity follows the behaviour of the solvent. After that,  $\eta$  evidences a single step increase, with  $T$ , that covers some orders of magnitude (about three for  $c = 0.32$ ). For the remaining concentrations, there is an additional step increase located in a different temperature range. For concentrations  $c > 0.43$ , the overall viscosity increase is of about five orders of magnitude. The first step increase in the L64/D<sub>2</sub>O micellar system is due to the percolation process that is characteristic of a colloid with a short-range attractive interaction [20]. The second step increase in  $\eta$ , reaching very large absolute values ( $> 10^3$  Pa), is located in the region where the KGT is observed [19]. Data of figure 3, in which the frequency dependence of  $G'(\omega)$  and  $G''(\omega)$  is reported for a given concentration ( $c = 50$  wt%) just for temperatures near the PT (22 °C) and in the vicinity of the KGT ( $T = 24.5$  °C), confirm that these two step increases in viscosity can be separately attributed to these transitions. In addition, from these data (figures 2 and 3) we have the clear signature that PT and KGT are located in different phase regions.

Near PT the moduli are characterized by a precise scaling behaviour with  $G''$  dominant over  $G'$ . This behaviour agrees with the universal scaling of percolation theory applied to complex



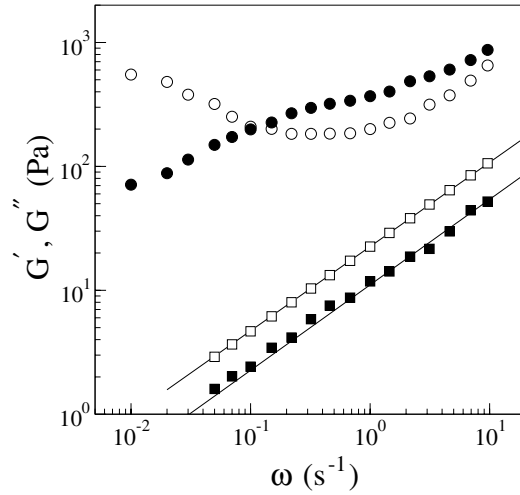


**Figure 3.** The frequency dependence of the shear moduli  $G'(\omega)$  (full symbols) and  $G''(\omega)$  (open symbols), at  $c = 50$  wt%, for  $T = 22^\circ\text{C}$  near the percolation transition (squares), and in the vicinity of  $T_c$ , at  $T = 24.5^\circ\text{C}$  (circles). As can be observed near the percolation threshold both are characterized by a precise scaling behaviour, whereas in the region of the glass transition  $G'$  dominates  $G''$  over a large  $\omega$  interval and presents an inflection point, where it varies very slowly with  $\omega$ , and  $G''$  evidences a marked minimum.

fluids that predicts for  $G'$  and  $G''$  a power-law dependence on  $\omega$  [25]:  $G' \approx G'' \approx \omega^\Delta$ .  $\Delta$  is an universal exponent with a expected value  $\Delta \sim 0.7$  [23]; we obtain  $\Delta = 0.67 \pm 0.05$  and  $\Delta = 0.68 \pm 0.05$ , for  $G'$  and  $G''$  respectively. On approaching the KGT the situation changes dramatically;  $G'$  begins to dominate  $G''$  over a large  $\omega$  interval, presents an inflection point, where it varies very slowly with  $\omega$ , and  $G''$  evidences a marked minimum. The inflection point in  $G'$  is located nearly at the frequency of  $G''_{\min}$ . An analogous situation was obtained in HS colloids on changing concentration [8]. The description of these frequency dependences of the shear moduli in terms of an MCT approach is our main objective.

Figure 2 evidences another interesting situation in the low-shear viscosity: its sharp reduction and its eventual flattening off at high temperatures (with  $\eta$  values of the order of few pascal). This phenomenon represents the clear evidence of the re-entry of the system into the liquid state (glass-to-liquid transition (GL)). The observed two-step increase in the viscosity (increasing  $T$ ), one for the PT and the other one for the KGT, have been recently investigated [26] in the frame of the results obtained in a Monte Carlo simulation of the slow dynamics in gelation phenomena [27]. In this latter work the connections among the colloidal gelation, the colloidal KGT and the classical gelation (as originally described by Flory) are described in a unifying way. The two-step behaviour is a manifestation of the colloidal short-range attraction in terms of the clustering and the SA process. Whereas at low concentration all the dynamics is governed only by the clustering that originates the gelation (the single step increase in  $\eta$  at low concentrations) at high concentration there is the onset of the SA, so that, in this concentration region, the system crosses over from colloidal gelation to colloidal glass due to the combined effects of clusters and particle jamming (the same picture invoked by MCT to explain the onset of the attractive glass). Only when the attraction is very strong the cluster effect will dominate and the slow dynamics will exhibit features closely related to the classical chemical gelation.

The observed viscoelasticity near the KGT temperature, i.e. the dominance of  $G'$  over  $G''$  and the minimum in  $G''$ , can be explained by using MCT. As is well known the main quantity in



this theory is the normalized density correlation function  $\phi_q(t) = \langle \rho_q^*(t) \rho_q \rangle / \langle |\rho_q|^2 \rangle$  detectable in a PCS experiment by the ISF [5]. MCT predicts a critical temperature  $T_c$  (and a critical concentration  $c_c$ ) where the ergodic to nonergodic transition takes place, and  $\phi_q(t)$  tends to the finite plateau  $f_q$  for  $t \rightarrow \infty$ . The separation parameter is  $\sigma \approx (T_c - T)/T_c$  (or  $(c_c - c)/c_c$ ). The theory proposes various density relaxation regimes with very different temporal scales. The short-time dynamics region  $t < t_0$  is dominated by microscopic motions, and is followed by the  $\beta$  relaxation region that satisfies the scaling relation

$$\phi_q(t) = f_q + h_q G(t) = f_q + c_\sigma h_q g_\pm(t/t_\sigma) \quad (1)$$

where  $f_q$  is the non-ergodicity parameter,  $h_q$  is the critical amplitude and  $G(t)$ , that includes the time dependence, is the so-called  $\beta$  correlator. The equation (1) form holds for all correlators between variables which have an overlap with density fluctuations. The correlator  $G$  depends singularly on the time and on the control parameter; this dependence is in two scales: an amplitude or a correlation scale  $c_\sigma = |\sigma|^{1/2}$  and the timescale  $t_\sigma = t_0 |\sigma|^{-1/2a}$ . The initial part ( $g_\pm(t \ll t_\sigma) = (t/t_\sigma)^{-a}$ ), dominated by  $t_\sigma$ , gives the approach to  $f_q$ , while the final one follows the von Schweidler law  $g_-(t_\sigma \ll t \ll t'_\sigma) = -h_q(t/t'_\sigma)^b$ , with  $t'_\sigma = t_0 |\sigma|^\gamma$  as the second characteristic timescale.  $\gamma = (1/2a) + (1/2b)$ .  $a$  ( $0 < a < 0.5$ ) and  $b$  ( $0 < b < 1$ ) are non-universal exponents determined solely by the so-called exponent parameter  $\lambda$  as  $\lambda = \Gamma^2(1-a)/\Gamma(1-2a) = \Gamma^2(1+b)/\Gamma(1+2b)$  where  $\Gamma$  is the Euler gamma function and  $\lambda$  is in turn determined by the static structure factor  $S_q$ . Finally, for  $t > t'_\sigma$  there is the  $\alpha$  relaxation regime.

For HS the values of the exponents are  $a = 0.301$  and  $b = 0.545$  [4, 5]. From our previous PCS experiment we have measured  $b = 0.6$  and  $\lambda = 0.7$ . In addition, a universal plot, for different ISFs, of the von Schweidler law gives  $\gamma = 2.3$ . MCT (and the explanation of  $\beta$  relaxations) was developed originally by using cage effects [4, 13] (or clustering) that determine the temporal (or frequency) dependence of relaxations. At very short times, density relaxation reflects the localized motion of individual particles, entailing the details of the hydrodynamic interactions. At longer times, particles are trapped in their neighbour structure. Below the glass transition, clusters can break up, making the system ergodic. By contrast, near and above  $T_c$  (or  $\phi_c$ ) clusters cannot break up and the system is non-ergodic. Changes in the cluster configuration provide the mechanisms for energy storage and dissipation, contributing to the moduli (i.e. stable clusters mean an elastic structure in which  $G'$  dominates). The time-dependent shear viscosity can be written as [28]

$$\eta(t) = \frac{k_B T}{60\pi^2} \int_0^\infty dq \left[ nq^2 \frac{d \ln S(q)}{dq} \phi(q, t) \right]^2 \quad (2)$$

where  $S(q)$  is the structure factor. The complex shear modulus  $\tilde{G}(\omega)$  is then given by the Laplace transform,  $\tilde{G}(\omega) = i\omega \int_0^\infty dt e^{i\omega t} \eta(t)$ , and in the region of the  $\beta$  density correlator it becomes a function of a scaled frequency variable  $\hat{\omega} = \omega t_\sigma$  corresponding to the scaled time variable  $\hat{t} = t/t_\sigma$

$$\tilde{G}(\omega) = k_B T [-g_0 + g_1 c_\sigma \tilde{\chi}(\hat{\omega}) + g_2 c_\sigma^2 \tilde{\psi}(\hat{\omega})] \quad (3)$$

where the coefficients are given by

$$g_0 = \frac{k_B T}{60\pi^2} \int_0^\infty dq \left[ q^2 \frac{d \ln S(q)}{dq} f(q) \right]^2 \quad (4)$$

$$g_1 = \frac{k_B T}{30\pi^2} \int_0^\infty dq \left[ q^2 \frac{d \ln S(q)}{dq} \right]^2 f(q) h(q) \quad (5)$$

$$g_2 = \frac{k_B T}{60\pi^2} \int_0^\infty dq \left[ q^2 \frac{d \ln S(q)}{dq} h(q) \right]^2 \quad (6)$$

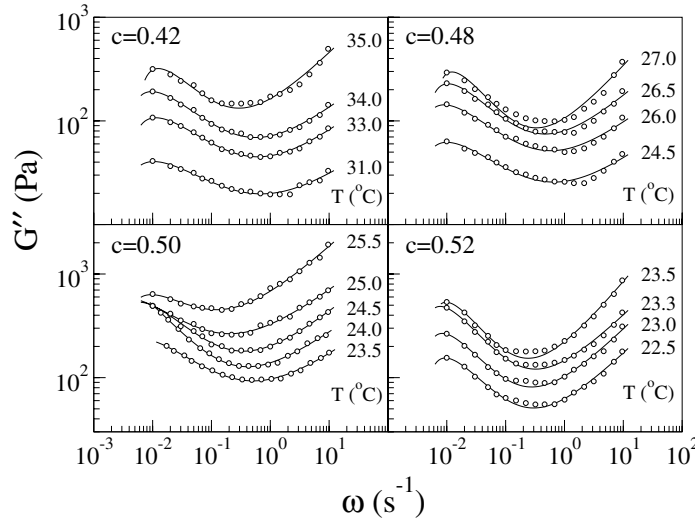


**Figure 4.** The loss shear moduli  $G''(\omega)$  as a function of frequency for different temperatures near the kinetic glass transition at four concentrations in the range  $0.42 < c < 0.52$ . The solid curves represent the corresponding MCT fits on approaching the structural arrest for which we get the values of the exponent parameter  $\lambda = 0.73, 0.70, 0.71$  and  $0.60$  respectively, all with an uncertainty of  $\pm 0.04$ .

and the susceptibilities are defined by

$$\frac{\tilde{\chi}(\hat{\omega})}{i\hat{\omega}} = \int_0^\infty d\hat{t} e^{i\hat{\omega}\hat{t}} g_-(\hat{t}), \quad \frac{\tilde{\psi}(\hat{\omega})}{i\hat{\omega}} = \int_0^\infty d\hat{t} e^{i\hat{\omega}\hat{t}} g_-^2(\hat{t}). \quad (7)$$

which are related by the MCT equation for the  $\beta$  correlator by  $\lambda\tilde{\psi}(\hat{\omega}) + \tilde{\chi}^2(\hat{\omega}) + 1 = 0$ . The final expressions for the storage modulus  $G'$  and the loss modulus  $G''$  are

$$\begin{aligned} G' &= -g_0 + g_1 c_\sigma \chi'(\hat{\omega}) \left[ 1 - \frac{g_2 c_\sigma}{\lambda g_1} \frac{1 + \chi'^2(\hat{\omega}) - \chi''^2(\hat{\omega})}{\chi'(\hat{\omega})} \right] \\ G'' &= g_1 c_\sigma \chi''(\hat{\omega}) \left[ 1 - \frac{2g_2}{\lambda g_1} c_\sigma \chi'(\hat{\omega}) \right]. \end{aligned} \quad (8)$$

When very close to the KGT, and to the lowest order in the control parameter  $\sigma$ , the shear moduli behave like the susceptibility and show the usual scaling properties. Our  $G'$  data are not accurate enough to allow fitting with MCT; we use the much more accurate measured values of  $G''$  using the amplitude parameters  $G_1 = g_1 c_\sigma$  and  $G_2 = 2g_2 c_\sigma / (\lambda g_1)$ , the frequency  $\omega_\sigma$  and the exponent parameter  $\lambda$ . According to the MCT the scaling in the  $\beta$ -correlation region implies the scaling of frequency and the loss modulus at the minimum. In particular, the  $\omega_{\min}$  position and the intensity of  $G''_{\min}$  depend sensitively on the control parameter; in particular, it is easy to express the two scales  $1/t_\sigma$  and  $G_1$  in terms of  $\omega_{\min}$  and  $G''_{\min}$  so that we also expect  $\omega_{\min} \approx |\sigma|^{1/2a}$  and  $G''_{\min} \approx |\sigma|^{1/2}$ .

The resulting fits are reported in figure 4, which shows  $G''$  for various temperatures on approaching the structural arrest at various concentrations,  $c = 0.42, 0.48, 0.50$  and  $0.52$ , for which we get the values of the exponent parameter  $\lambda = 0.73, 0.70, 0.71$  and  $0.60$  respectively, all with an uncertainty of  $\pm 0.04$ . Figure 5(a) reports  $\omega_{\min}^{2a}$  as a function of  $T_c - T$  for the different concentrations we studied (nearly the same as used in our previous PCS experiment [16]). As can be observed the linear law for  $\omega_{\min}^{1/2a}$  in  $T_c - T$  is well verified and gives an indication of

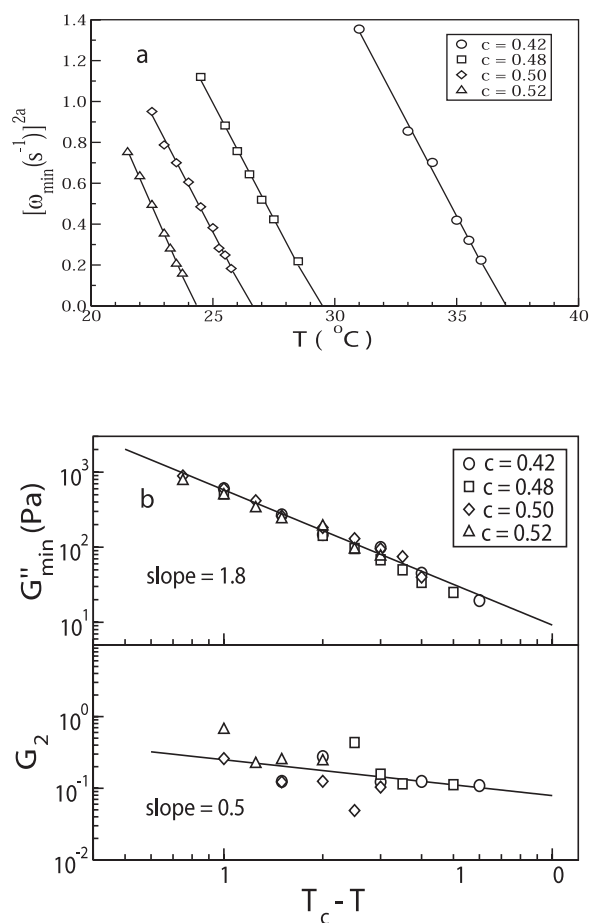


**Figure 5.** (a) The power-law dependence of  $\omega_{\min}^{2a}$  on  $T$  for different micellar concentrations. Solid lines represent data fits. (b) The parameters for the loss modulus  $G''$  as a function of the distance from the temperature of structural arrest.

the glass transition temperatures as  $T_c = 36.95, 29.45, 26.55$  and  $24.29^{\circ}\text{C}$ , very close to the experimentally determined values within  $\pm 0.2^{\circ}\text{C}$ . Using these values for the glass transition temperature, we can check the power laws for the other two parameters,  $G''_{\min}$  and  $G_2$ , and obtain the slopes 1.8 and 0.5 respectively, as shown in figure 5(b). MCT predicts the value 0.5 for both exponents. While  $G_2$  has the correct value, the slope for  $G''_{\min}$  is much higher than expected, a result similar to the one observed experimentally in HS systems [8]. Contrary to that case, we do not need to include the high-frequency contribution that was calculated for HSs.

A comment on the values of  $\lambda$  is in order. The almost constant value around 0.7 for the lower values of the concentration indicates a set of measurements along the attractive glass line, while the lower value at  $c = 0.52$  indicates vicinity to a repulsive glass transition. In fact, near an attractive glass transition line the parameter  $\lambda$  is slowly varying, while it has a steep variation close to a repulsive glass line [10]. This interpretation of the data is in agreement with the previous PCS measurements [18] and the more recent neutron scattering experiments [17, 19]. The overall picture seems to conform to the predictions of MCT when applied to short-range attractive colloids.

Apart from the frequency dependence of the amplitude of  $G''$ , we have a good agreement between the two independent measurements, the actual rheological and the previous light scattering one. This is an important confirmation of the validity of the MCT approach in the analysis of viscoelasticity parameters in the region of the KGT. Even if we believe it to be in the region of the phase diagram close to the attractive glass transition line, the effect of the close higher-order singularity of type A3 is not present in the frequency region we studied. Such an effect is instead dramatic in PCS experiments [16, 18] where a logarithmic slowing down shows up in the ISF due to the singularity. In the case of the loss modulus we would expect a frequency-independent behaviour at low frequencies [13].

#### 4. Conclusion

In conclusion, we have shown that the frequency-dependent viscoelastic shear moduli, in a micellar system with adhesive interactions, are strongly modified as the temperature approaches both the percolation and the structural arrest at the glass transition. These processes, entirely due to clustering effects originating from the interparticle attraction, have been studied in the system phase diagram where they appear as two separate lines, both temperature–composition dependent. At a fixed concentration (increasing the temperature) the dynamical effects of these two transitions are reflected in system low-shear viscosity with a two-step increase that covers many orders of magnitude. The physical origin of this behaviour lies in the combined effects of clustering (originating the PT) and particle jamming (that give rise to the KGT) that originates the observed crossover from colloidal gelation (first viscosity step) to colloidal glass (second step). At the gelation the frequency dependence of the shear moduli is described in terms of a percolation approach; both  $G'(\omega)$  and  $G''(\omega)$  obey a scaling law. At the KGT we observed for the loss moduli  $G''(\omega)$  (studied at different concentrations as a function of temperature) a universal behaviour, well explained by the application of MCT approaches, only partly different from the analogous ones used for HS colloids. The values of the measured MCT parameters agree well with the results of a previous study on the same system by using light scattering and partially confirm the predicted theoretical effects of the attraction on the KGT [7, 9, 11], previously described.

#### Acknowledgments

The MIT research is supported by a grant from the Materials Science Division of USDOE. The research in Italy is supported by the INFM-HOP and MURST-PRIN2000. We also acknowledge the support of the European Community Marie Curie Network ‘Dynamical arrest’, contract no MRTN-CT-2003-504712.

#### References

- [1] Everett D H 1988 *Basic Principles of Colloid Science* (Letchworth: Royal Society of Chemistry)
- [2] Baxter R J 1968 *J. Chem. Phys.* **49** 2770
- [3] Chen S H, Rouch J, Sciortino F and Tartaglia P 1994 *J. Phys.: Condens. Matter* **6** 10885
- [4] Götze W 1991 *Liquids, Freezing and the Glass Transition* ed J P Hansen, D Levesque and J Zinn-Justin (Amsterdam: North-Holland)
- [5] van Meegen W and Underwood S M 1993 *Phys. Rev. Lett.* **70** 2766  
van Meegen W and Underwood S M 1994 *Phys. Rev. E* **49** 4206
- [6] Cates M E, Wittmer J P, Bouchaud J-P and Claudin P 1998 *Phys. Rev. Lett.* **81** 1841
- [7] Liu A J and Nagel S R 1998 *Nature* **396** 6706
- [8] Mason T G and Weitz D A 1995 *Phys. Rev. Lett.* **75** 2770

- [9] Dawson K 2002 *Curr. Opin. Colloid Interface Sci.* **7** 218
- [10] Fabbian L, Götz W, Sciortino F, Tartaglia P and Thiery F 1999 *Phys. Rev. E* **59** R1347  
Dawson K A *et al* 2000 *Phys. Rev. E* **63** 11401
- [11] Bergenholtz J and Fuchs M 1999 *Phys. Rev. E* **59** 5706
- [12] Bartsch E, Antonietti M, Shupp W and Sillescu H 1992 *J. Chem. Phys.* **97** 3950
- [13] Sjögren L 1991 *J. Phys.: Condens. Matter* **3** 5023
- [14] Eckert T and Bartsh E 2002 *Phys. Rev. Lett.* **89** 125701
- [15] Pham K N, Puertas A M, Bergenholtz J, Egelhaaf S, Moussaid A, Pusey P N, Schofield A B, Cates M E, Fuchs M and Poon W C K 2002 *Science* **296** 104
- [16] Mallamace F, Gambadauro P, Micali N, Tartaglia P, Liao C and Chen S H 2000 *Phys. Rev. Lett.* **84** 5431
- [17] Chen W R, Chen S H and Mallamace F 2002 *Phys. Rev. E* **66** 021403
- [18] Chen W R, Chen S H and Mallamace F 2003 *Science* **300** 619
- [19] Chen W R, Mallamace F, Glinka C J, Fratini E and Chen S H 2003 *Phys. Rev. E* **68** 041402
- [20] Lobry L, Micali N, Mallamace F, Liao C and Chen S H 1999 *Phys. Rev. E* **60** 7076
- [21] Flory P J 1953 *Principles of Polymer Chemistry* (Ithaca, NY: Cornell University Press)
- [22] Verduin H and Dhont J K G 1995 *J. Colloid Interface Sci.* **172** 425
- [23] Del Gado E, de Arcangelis L and Coniglio A 2000 *Eur. Phys. J. E* **2** 359
- [24] Martin J E, Wilcoxon J and Odinek J 1991 *Phys. Rev. A* **43** 858
- [25] de Gennes P-G 1979 *Scaling Concepts in Polymer Physics* (Ithaca, NY: Cornell University Press)
- [26] Mallamace F, Coniglio A, Del Gado E and Chen S H 2004 at press
- [27] Del Gado E, Fierro A, de Arcangelis L and Coniglio A 2003 *Europhys. Lett.* **63** 1
- [28] Bengtzelius U, Götz W and Sjölander A 1984 *J. Phys. C: Solid State Phys.* **17** 5915